Supplementary Information to

Radio frequency radiation-induced hyperthermia using Si-nanoparticle-based sensitizers for mild cancer therapy

Konstantin P. Tamarov[1], Liubov A. Osminkina[1], Sergey V. Zinovyev[2], Ksenia A. Maximova[3], Julia V. Kargina[1], Maxim B. Gongalsky[1], Yury Ryabchikov[3], Ahmed Al-Kattan[3], Andrey P. Sviridov[1], Marc Sentis[3], Andrey V. Ivanov[2], Vladimir N. Nikiforov[1], Andrei V. Kabashin[3], and Victor Yu. Timoshenko[1]

[1]*Moscow State Lomonosov University, Department of Physics, 119991 Moscow, Russia*
[2]*Russian Cancer Research Blokhin Center, 115478 Moscow, Russia*
[3]*Aix Marseille University, CNRS, LP3 UMR 7341, Campus de Luminy - Case 917, 13288, Marseille Cedex 9, France*

1. Structural Characterization of Nanoparticles

Structural properties of porous silicon (PSi) nanoparticles (NPs) were studied by measuring adsorption/desorption isotherms of nitrogen. Aqueous suspensions of PSi NPs were obtained by high-energy milling of electrochemically prepared PSi layers in distilled water. Prior the measurements the suspensions were freeze-dried by lyophilisation process for 3 h in order to obtain powder of PSi NPs. The surface area of PSi NPs and their pore size distribution were evaluated by using the Brunauer-Emmett-Teller (BET) and Barret-Joyner-Halenda (BJH) methods, respectively. Fig. S1 shows typical adsorption-desorption curve and pore size distribution, which reveal mesoporous structure of the investigated NPs.

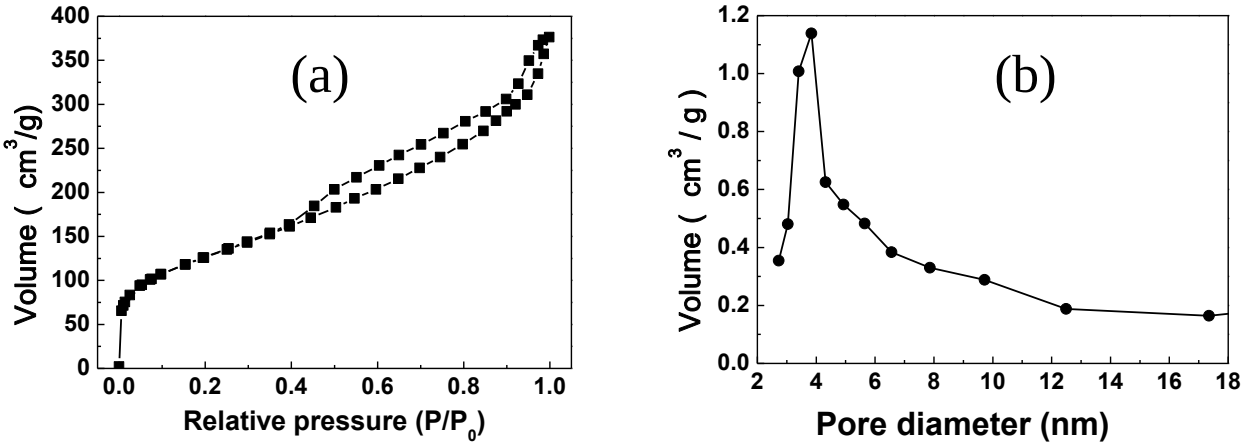

Figure S1. (a) Nitrogen adsorption/desorption isotherm and (b) pore size distribution in dried PSi NP powder

Fig. S2 shows typical infrared (IR) transmission spectra of dried PSi NPs deposited on double side polished crystalline Si wafer. The IR transmission of the latter was used as the background. Here, the absorption peak of vibrational Si-O-Si mode (1070 cm^{-1}) reveals a strong oxidation of freshly prepared PSi. However, a bit of hydrogen remains on the PSi NPs surface, which is evidenced by the presence of absorption peaks of Si-H stretching modes of O-Si-H_x (x=1,2,3) bonds at 2082-2190

cm^{-1}. A decrease of the IR transmittance in the spectral region of Si-O-Si vibrational modes (1000-1150 cm^{-1}) for PSi NPs after RF irradiation in suspension can be explained by additional oxidation of NP surface due to the RF induced heating.

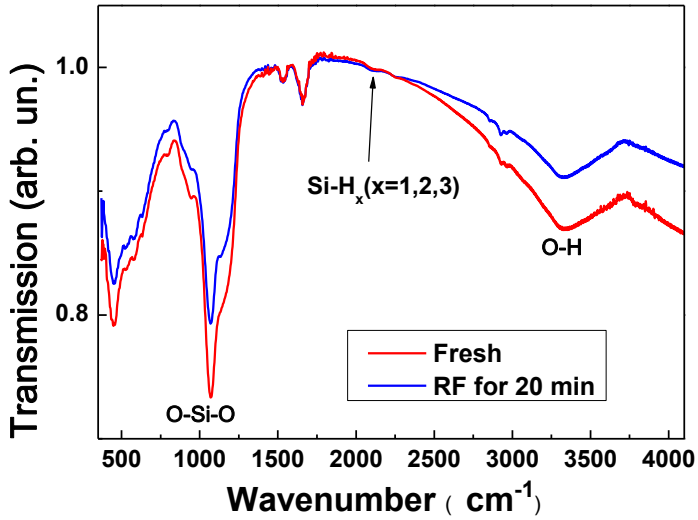

Figure S2. IR transmission spectra of dried PSi NPs before (blue curve) and after (red curve) the RF irradiation at 5 W/cm^2 for 20 min.

For comparison, we also prepared Si and Au NPs by laser ablation in deionized water (they will later be denoted as LA-Si and LA-Au NPs). As shown in Fig. S3(a), the LA-Au NPs are nanocrystalline (see the electron diffraction pattern in the inset of Fig. S3 (a)) and have nearly spherical shape. The size distribution of LA-Au NPs is centered at 20 nm (see Fig. S3 (b)).

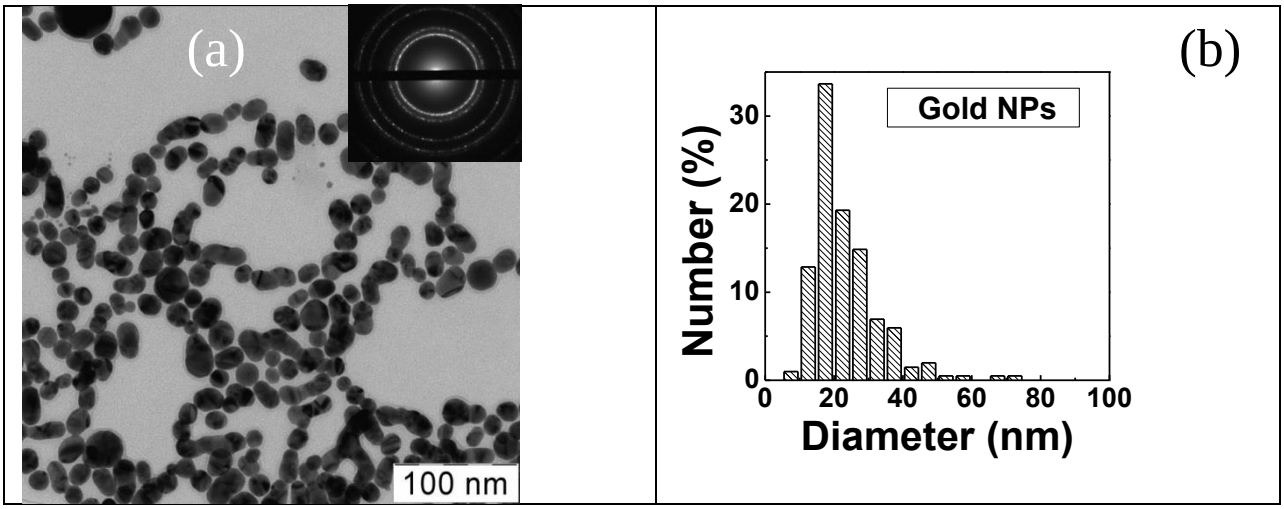

Figure S3. (a) TEM image of LA-Au NPs and corresponding diffraction pattern in the inset; (b) size distribution of LA-Au NPs obtained from the TEM image

2. Water solubility of laser-ablated Si NPs

The water-solubility and biodegradability of PSi NPs is well studied in the literature (see e.g., Ref. 13 of the manuscript). In our tests, we examined the solubility of laser-ablated Si nanoparticles in aqueous solutions using TEM and Raman spectroscopy. Aqueous suspensions of LA-Si NPs with

initial concentration of 0.5 mg/mL were diluted with physiological solution (0.9 % NaCl) at the ratio of 1:1. The prepared mixture (1 mL) was put into a dialysis vessel, which was introduced into large amount (5L) of de-ionized water with fixed pH level of 7.0 at room temperature (20-22 C). The experiment was carried out in a dark room to avoid any photoexcitation effects. Droplets of liquids were taken from the vessel after different times of the dissolution experiment and dropped onto carbon-coated TEM grids. TEM images of LA-Si NPs and corresponding size distributions in the as-prepared suspension and those after 5 days storage are shown in Fig. S4 (a, b), respectively. One can see a drastic decrease of the mean nanoparticle size from 30 to 10 nm and a complete disappearance of relatively large NPs (> 20 nm) just 5 days after the beginning of the test. It is clear that the observed decrease of the nanoparticle size can only be explained by dissolution of LA-Si NPs similarly to how it took place in Ref. 13.

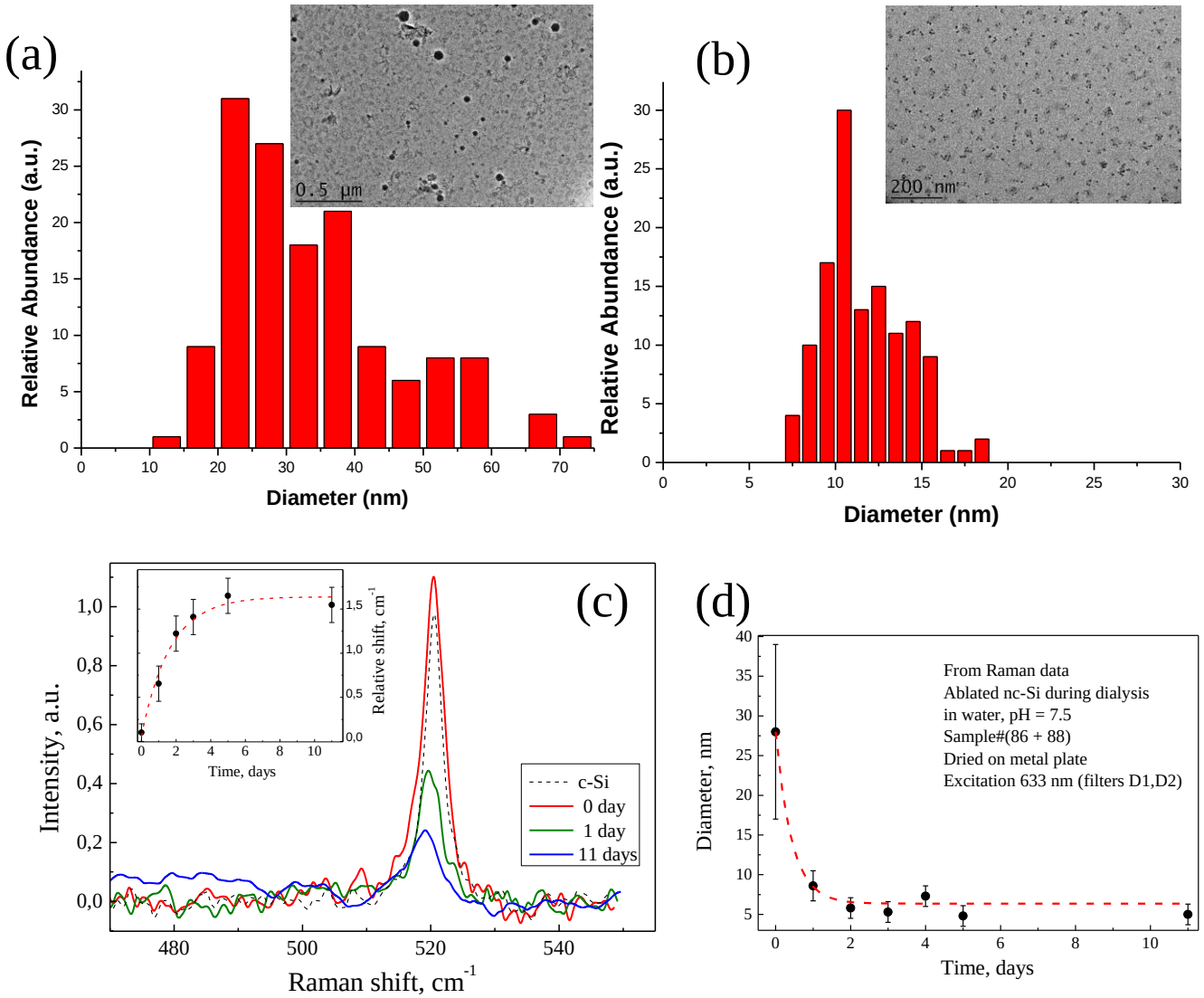

Figure S4. TEM images (insets) and corresponding size distributions of LA-Si NPs in deionized water at the initial concentration of 0.5 mg/mL: (b) as prepared nanoparticles; (c) after 5 days of their storage in the physiological solution. (c) Evolution of Raman spectra from LA- Si NPs for different durations of their storage in the physiological solution. The inset shows the evolution of the Raman peak position; (d) Mean size of LA-Si NPs estimated from Raman spectra

The dissolution process was independently studied by Raman spectroscopy under the same dialysis conditions. Droplets containing LA-Si NPs were taken from the solution at different moments after the beginning of the dissolution test, deposited on a metal plate and dried in air. The NPs were then tested by using a micro-Raman spectrometer under excitation with a HeNe laser at 633 nm. As shown in Fig. S4c, Raman spectra of the samples exhibited a peak near 520 cm^{-1} associated with the presence of crystalline Si NPs. The position of the peak shifted from 521 cm^{-1} to shorter wavenumbers (519-520 cm^{-1}) after several days of the dissolution process: such a shift is typically attributed to the decrease of the nanoparticle size. In this case, the size of Si nanocrystals can be estimated from the positions of Raman peaks using the well known phonon confinement model (see for example Ref. [1]). Results of such estimations are shown in Fig. S4d. One can see that the mean size of nanoparticles drops from 30 nm to less than 5 nm a few days after the beginning of the experiment, which roughly corresponds to results of TEM measurements (Fig. S4a,b). It should be noted that such Raman spectroscopy cannot precisely follow the size evolution of NPs if they become too small (< 5 nm).

3. RF heating of aqueous suspensions of NPs

Fig. S5 illustrates an increase of the temperature of aqueous suspension of LA-Au NPs with concentration of 50 *μg/mL* under the RF irradiation with intensity of 5 W/cm^2. The corresponding heating rate is estimated to be about 1.4 K/min.

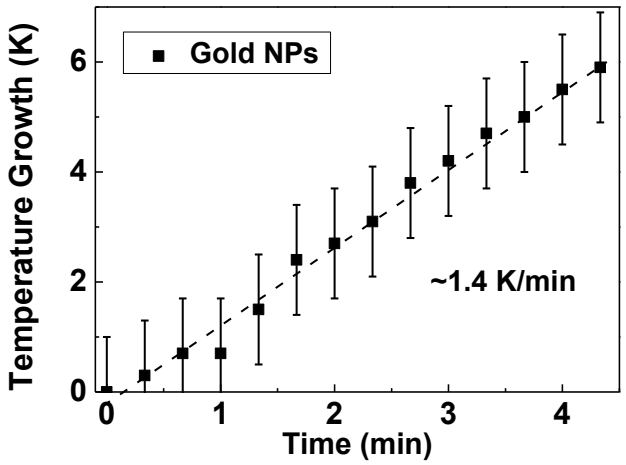

Figure S5. Heating of 20 *mL* aqueous suspension of LA-Au NPs with concentration of 50 μg/mL under RF irradiation with the intensity of 5 W/cm^2. The initial temperature of the suspension was 22^oC.

Fig. S6 shows time dependences of the temperature increase of aqueous suspension of LA-Si NPs prepared by laser ablation of lightly (specific resistivity of 1-10 Ohm*cm) and heavily (specific resistivity of 10-15 mOhm*cm) boron doped c-Si wafers for the RF irradiation with intensity of 5 W/cm^2. The concentration of LA-Si NPs was 30 ±5 *μg/mL* for the both samples. The heating rate estimated for the initial linear part of the dependence account 0.8±0.1 and 0.9±0.1 K/min for the samples ablated from lightly and heavily doped c-Si, respectively. This small difference in the heating rate for the sample prepared from lightly and heavily doped c-Si is within error bars related to the measured NP concentration and suspension temperature.

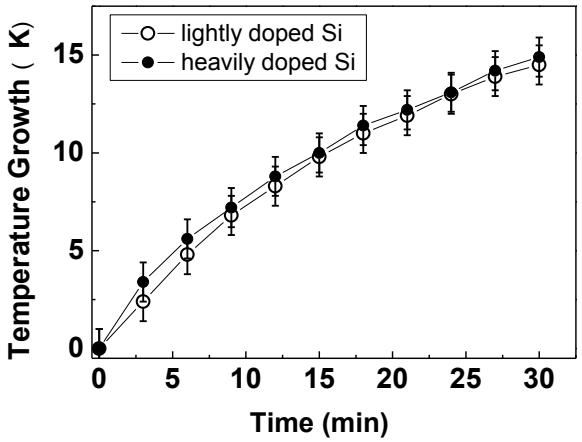

Figure S6. Time dependence of the RF irradiation induced temperature of 20 *mL* aqueous suspensions of LA-Si NPs produced by laser ablation of lightly (open circles) and heavily (close circles) boron doped c-Si wafers. The RF radiation intensity was 5 W/cm^2 and the initial temperature of the both suspensions was 22°C.

4. In vitro toxicity of Si NPs.

Hep2 (laryngeal cancer cells) were used for the evaluation of cytotoxicity of PSi and LA-Si NPs. The prepared aqueous suspensions were mixed with DMEM (BioloT, Russia) in the ratio of 1:1, and then the mixtures were added to the cell culture and were incubated for 24 h. The reference cell group was incubated in DMEM. The cell viability was evaluated by using a hemocytometer. Living and dead cells were separated by their coloring with Trypan Blue (Paneco-ltd, Russia). The results were statistically processed using Student's t-test with certainty 0.95. As shown in Fig. S7, LA-Si NPs demonstrate "zero" toxicity and do not influence Hep2 proliferation for the whole range of NPs concentrations (< 0.06 mg/mL), while Psi NPs demonstrate similar results until very high concentrations (0.6-0.7 mg/mL). Notice that a slight difference between the absolute values of the ratio in the left and right images can be explained by taking into account that cell cultures for the experiments were taken at different (but close) points of cell proliferation curve.

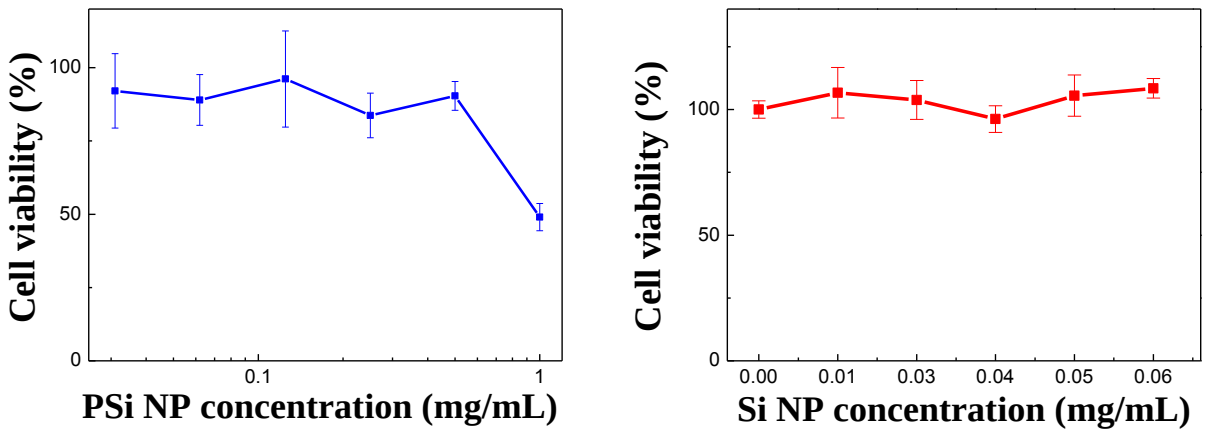

Figure S7. Concentration dependences of the viability of Hep-2 cells with added PSi (left) and LA-Si (right) NPs

5. In vitro assessment of the efficiency of RF-based treatment using Si NPs as sensitizers.

An effect of Si NPs and RF radiation was investigated with 3T3 cells. Aqueous suspensions of PSi and LA-Si NPs were diluted with PBS solution at the ratio of 1:1. The final concentrations of PSi and LA-Si were 0.5 mg/mL and 0.1 mg/mL, respectively. The prepared mixtures were added to the of 3T3 cells, which were removed from the substrates by a standard trypsinization procedure. Prior the RF experiments the mixtures of NPs and cells were stored in darkness for 20 min. The reference cells without NPs were also investigated for comparison. The cells were treated by RF irradiation with intensity of 2 W/cm^2 for 4 min. After the treatment the cells were put into Petri dishes and incubated for 24 h.

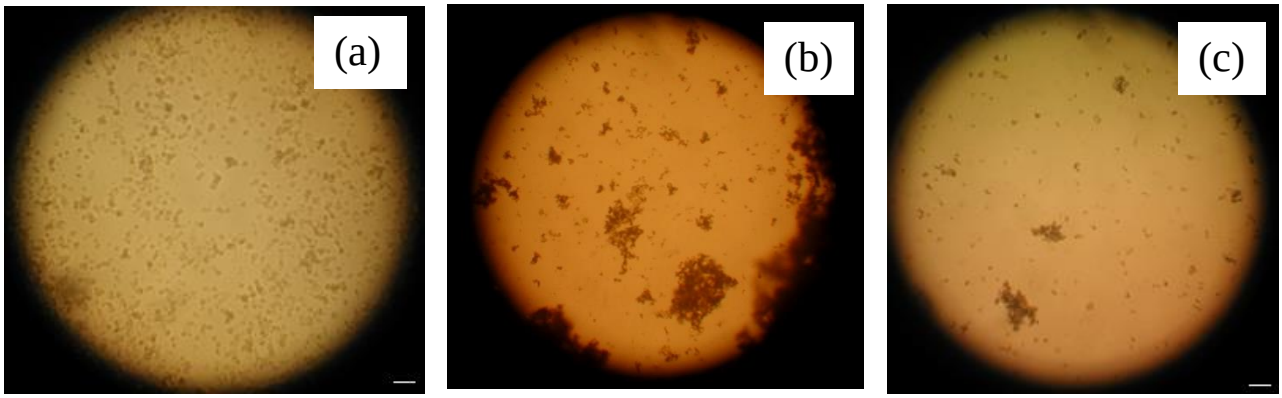

Figure S8. Optical large-scale images of 3T3 cells after RF irradiation (4 min, 2 W/cm^2) and (b) the cells loaded with PSi NPs (0.5 mg/mL) followed by the RF irradiation; (c) the cells loaded with LA- Si NPs (0.1 mg/mL) followed by the RF irradiation. The scale bars correspond to 100 μm

Our experiments showed that in the absence of Si NPs the action of RF radiation with the chosen parameters did not lead to a remarkable elimination of cancer cells with the estimation of the survival rate of about 90-95%. A typical image of 3T3 cells after the treatment is shown in Fig. S8a. However, a preliminary loading of the cells by NPs radically changes the efficiency of RF-based treatment yielding to the drastic cell elimination. Applying RF radiation of the same intensity, we recorded the survival rate of less than 12% and 10% for PSi and LA-Si NPs, respectively. Typical images of cell colonies loaded with PSi or LA-Si NPs after RF treatment are shown in Fig. S8 (b) and (c), respectively. It is visible that the RF treatment led to almost complete elimination of cells, while liberated NPs linked to large agglomerations after the treatment procedure.

6. Effect of Si nanoparticles on the blood content

Wistar rats (male and female) of mass 150±20 g were intragastrically injected with water suspensions of PSi and LA-Si NPs of dose 0.7 mg/kg. Rats in the control group were similarly injected with distilled water of the same volume. The content of the studied biochemical parameters was determined in blood plasma of experimental animals after a single or sevenfold administration of Si NPs. The animals were sacrificed after 24 hours after the last measurement. The activity of aminotransferase was determined by Reitman-Frankel method (ALT, AST). The activity alkaline phosphatase (ALP) was measured by kinetic method from the increase of coloring of p-nitrophenol in diagnostic kits LaChema (Czech Republic). The cholesterol content was determined by a kinetic

method. The concentration of unconjugated and conjugated bilirubin (UB, CB) was determined by Malloy-Evelyn method using VitalDiagnostics kits (Russia) and biochemical analyzer Chem Well (USA). All parameters were compared for the control group and the groups injected with NPs. Statistical analysis of the results was performed using Student's t-test.

The biochemical analysis of blood plasma of the experimental animals injected with PSi and LA-Si NPs did not reveal any significant changes in the blood content. The intragastric administration (single or seven-fold) of PSi and LA-Si NPs at the dose of 0.7 mg/kg did not significantly affect the maintenance of transaminase, alkaline phosphatase, bilirubin and cholesterol in blood. The obtained biochemical data were the same for different rat genders. Tables 1 and 2 show the average results of the content of individual cells markers of cytolysis (ATL and AST) during measurement of blood plasma samples. Here, only minor changes of the investigated parameters can be found. Comparing the data of tables 1 and 2, one can notice that a single administration of PSi NPs induced a slight increase of aminotransferase content in plasma. Although this effect was not significant after sevenfold administration, AST/ALT ratio increased up to 1.5 ± 0.1.

Table 1. Effect of Si NPS on the content of ALT and AST in the rats blood plasma after a single administration

Rat group	ALT, μkat/l	AST, μkat/l	AST/ALT ratio
Control	0.189±0.01	0.231±0.01	1.2±0.1
LA-Si	0.163±0.01*	0.21±0.01*	1.3±0.1*
PSi	0.234±0.01*	0.327±0.02*	1.4±0.1*

*P>0.05

Table 2. Effect of Si NPS on the content of ALT and AST in the rats blood plasma after a sevenfold administration

Rat group	ALT, μkat/l	AST, μkat/l	AST/ALT ratio
Control	0.252±0.01	0.288±0.01	1.1±0.1
LA-Si NPs	0.163±0.01*	0.21±0.01*	1.3±0.1*
PSi	0.174±0.01*	0.271±0.01*	1.5±0.1*

*P>0.05

Table 3. Effect of Si NPS on the content of cholesterol, bilirubin and alkaline phosphatase in the rats blood plasma after a single administration

Rat group	Cholesterol, mmol/l	CB, μmol/l	UB, μmol/l	CB/UB, %	ALP, U/l
Control	1.8±0.1	1.6±0.1	2.2±0.2	73±1.7	484±24
LA-Si NPs	2.0±0.1*	0.7±0.1*	0.8±0.1*	88±1.7*	512±25*
PSi	1.6±0.1*	1.4±0.1*	2.1±0.2*	67±1.6*	529±25*

*P>0.05

Table 4. Effect of Si NPS on the content of cholesterol, bilirubin and alkaline phosphatase in the rats blood plasma after a sevenfold administration

Rat group	Cholesterol, mmol/l	CB, μmol/l	UB, μmol/l	CB/UB, %	ALP, U/l
Control	1.9±0.1	2.5±0.2	2.8±0.2	89±1.8	489±24
LA-Si NPs	1.8±0.1*	0.9±0.1*	1.4±0.1*	64±1.6*	537*±26
PSi	1.7±0.1*	1.0±0.1*	1.3±0.1*	77±1.7*	504*±25

*P>0.05

Table 3 and 4 present data on the content of cholesterol, bilirubin and alkaline phosphatase. One can see that Si NPs did not induce significant changes in cholesterol and bilirubin concentrations after 24 hours after single administration but induced minor reduction after sevenfold administration, while seven-fold administration led to a slight decrease of these parameters. The analysis of plasma samples from groups injected with PSi and LA-Si NPs also reveals a slight increase in alkaline phosphatase concentration.

In summary, the intragastric administration of aqueous suspensions of PSi and LA-Si NPs into Wistar rats in dosages 0.7 mg/kg and 4.9 mg/kg does not cause any statistically significant changes in blood levels of aminotrasferases, alkaline phosphatase, bilirubin and cholesterol.

7. Results of in vivo RF treatment tests

Fig. S9 shows dependences of the tumor volume for different groups of animals, i.e. (a) intact mice (sterile water was intratumorally injected); (b) mice after intratumoral injection of 0.5 mL of aqueous suspension of PSi NPs with concentration of 1 mg/mL; (c) mice after 2 min of the RF irradiation with intensity of 2 W/cm^2; d) mice after intratumoral injection of 0.5 mL aqueous suspension of PSi NPs with concentration of 1 mg/mL followed with the RF irradiation with intensity of 5 W/cm^2 for 3 minutes. The initial volume of tumor, V_0, was in the range from 180 to 230 mm^3.

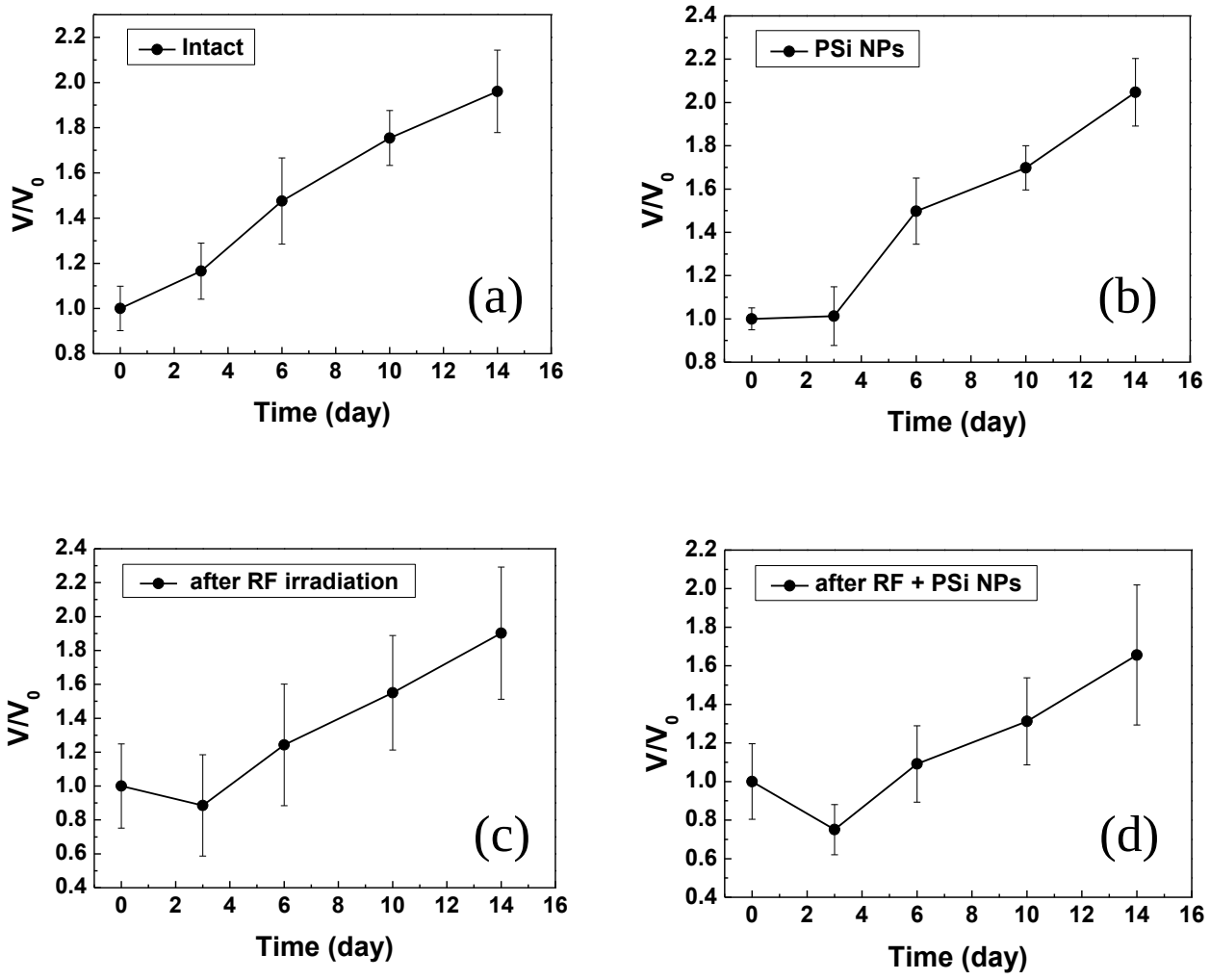

Figure S9. Time dependence of the relative tumor volume for the following groups of mice: (a) intact; (b) after intratumoral injection of 0.5 *mL* PSi NPs at 1 *mg/mL*; (c) after 2 *min* of the RF irradiation with intensity of 2 W/cm^2 and (d) combined action of the PSi NP injection (0.5 *mL*, 1 *mg/mL*) and RF irradiation. The 0 day of experiment corresponds to the PSi NPs injection and/or RF exposure.

8. Mice viability tests after RF treatment (intratumoral injection)

Mice of CBA line were divided into: (i) a reference group; and (ii) a group with intratumorally injected LA-Si Si NPs combined with RF irradiation. The reference group was administered with the equal volume of PBS buffer and RF radiation. Fig. S10 shows the mice viability for the two groups investigated. It can be seen that combined action of ablated Si NPs and RF radiation increased mice lifetime by 20-25%.

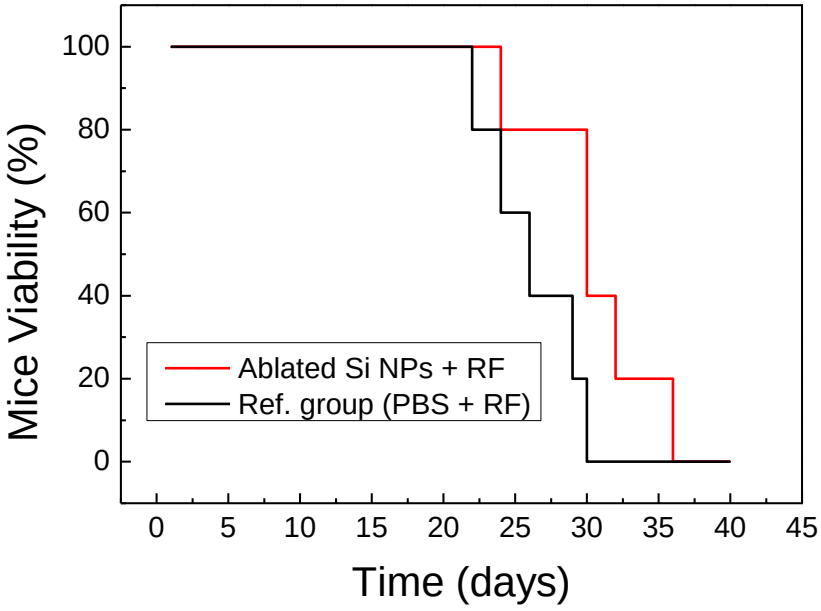

Figure S10. CBA line mice viability for two groups: reference group intratumoral injection of PBS and 2 min of the RF irradiation with intensity of 2 W/cm^2 (blue), and combined effect of LA-Si NPs and RF radiation (black).

9. Mice viability tests (intravenous injection)

We carried out a series of additional experiments on mice viability using intravenous injection of laser-ablated and PSi NPs. In order to improve the transport of NPs in the blood stream and to avoid the immune response, NPs are typically covered by biocompatible polymers. In our case dextran was selected as the model polymer. The particles were covered by physical adsorption of dextran on the surface of Si NPs. Possible effects of intraveneous injection of Si NPs were explored for BDF1 male mice with weighting 21–24 g. Both healthy mice and ones with cancer tumors (B16 melanoma) were divided into four groups (5 animals per group), i.e. two experimental groups and two reference ones. NPs were administered by single injection of a dose of 10, 20 or 30 mg/kg in a volume of 0.2 mL per mouse in its tail vein. The tolerance of NPs for healthy mice was evaluated over a period of 14 days after the administration by analyzing the state and behavior of mice including local reactions and death. The administration was considered to be tolerable if there were no irreversible side effects and the death of mice was not caused by the intoxication. Doses of 10, 20 and 30 mg/kg of PSi and LA-Si NPs were found to be tolerant for the healthy mice investigated. Furthermore, for LA-Si NPs we observed a significant increase of mice viability (by 20%), although the mechanism of this phenomenon is not yet clear for us and requires further investigation. This result is shown schematically in Fig. S11.

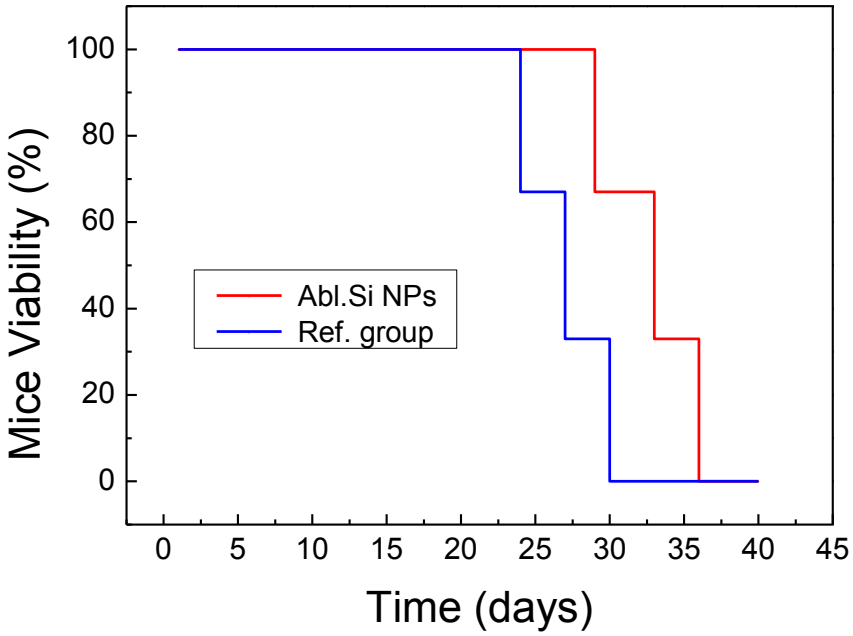

Figure S11. Dependences of the mice viability for the group with cancer tumor and intraveneously injected LA-Si NPs (red line) and for the reference group with cancer tumor (blue line).

[1] V. Pailard et al. J Appl. Phys. 86, 1921(1999)